

One-dimensional quantum rotator in solids: The para-ortho transition of H_2S^- in KCl

Dirk Schoemaker, Jin Fu Zhou,* and Etienne Goovaerts

Department of Physics, University of Antwerp (Universitaire Instelling Antwerpen), B-2610, Wilrijk (Antwerp), Belgium

(Received 18 July 1985)

Trapping of a mobile interstitial hydrogen atom by a substitutional SH^- impurity in KCl leads to the formation of a H_2S^- molecule on an anion site whose electron-spin-resonance (ESR) spectra exhibit axial symmetry around a $\langle 111 \rangle$ direction. A singlet line and a hydrogen hyperfine triplet both exhibiting the $\langle 111 \rangle$ symmetry but possessing slightly different g parameters are shown to belong to this H_2S^- center, and an Arrhenius analysis of the ESR intensities establishes that the triplet is excited at the expense of the singlet with a 16.2-cm^{-1} activation energy. From this and from an analysis of the g and ^{33}S hyperfine components incorporating higher-order corrections it is concluded that the H_2S^- molecule exhibits free or weakly hindered quantum rotation around its $\langle 111 \rangle$ -oriented C_{2v} axis: The proton-spin statistics only permit the nuclear singlet in the symmetric rotational ground state, while only the triplet nuclear state is allowed in the first-excited rotational state at 16.2 cm^{-1} . As a corollary to this investigation, a vexing problem about the structure of the substitutional S^- center is settled. Furthermore, the isotropic part of the hyperfine interaction of the free $\text{S}^-(3p^5)$ ion is shown to be large and negative. Data on D_2S^- and HDS^- centers are also presented.

I. INTRODUCTION

Reorientation motions of molecules on lattice sites in solids can vary from classical thermally activated jumping motions between equivalent orientations to quantum-mechanical free rotation. In between stand the tunneling and phonon-activated tunneling motions.¹ In the classical regime the reorientation rates are strongly temperature dependent and the motion of the molecule can vary from standing still to, depending on the activation energy and the stability of the molecule and/or the crystal, average reorientation rates approaching the quantum rotation frequency of the free molecule, i.e., the frequency corresponding to the first rotational transition of the free molecule. An interesting recent example is CN^- in the alkali cyanides, whose average thermally activated reorientation rate approaches the free rotation frequency just at the phase transition temperatures.² A glance at the literature reveals that thermally activated motion is a common occurrence.

Genuine free rotation of molecular solids is much less common. When it occurs it usually involves small compact molecules. A celebrated example is H_2 in solid molecular hydrogen, which, even at very low temperatures, exhibits essentially unhindered rotation.³ This is proven, e.g., by the observation in solid hydrogen of sharp rotational Raman lines at the free H_2 rotation energies. Another consequence of the free rotation is the existence of the para and ortho modification of molecular hydrogen, the origin of which is the interdependence of the nuclear-spin states and the molecular rotational states imposed by the nuclear-spin statistics.^{3,4} However, observing para and ortho states in molecules (or analogous states for cases where more than two identical nuclei are involved⁴) does not necessarily imply free rotation: Nuclear permutation symmetry is equally important when mole-

cules exhibit hindered rotation or tunneling motions. Cases in point are, e.g., the⁵ CH_3 and⁶ NH_2 radicals in solids, where the effect of the nuclear-spin statistics is readily observed in electron-spin resonance (ESR).⁷ These species are considered to be *hindered* quantum rotators at very low temperatures. Other examples of the latter are the substitutional⁸ NO_2 and⁹ N_2^- impurities in the alkali halides.

In the present paper we discuss the quantum rotation of a H_2S^- molecule in KCl. This system was discovered in the course of our Raman scattering and ESR investigations on hydrogen-atom (H^0) centers in $\text{KCl}:\text{SH}^-$ crystals.¹⁰ It was realized subsequently that the two ESR spectra that we will discuss in this paper had been observed earlier, but that their interpretation had been ambiguous and incomplete.¹¹ Specifically, one spectrum was attributed (erroneously as we will show) to a S^- center possessing $\langle 111 \rangle$ symmetry and the other to a H_2S^- molecule ion possessing the same symmetry. This has led to considerable confusion¹²⁻¹⁴ because the existence of a S^- center possessing $\langle 110 \rangle$ symmetry was also convincingly established in the alkali halides.¹⁵ We will show (Sec. III) that the two $\langle 111 \rangle$ ESR spectra clearly originate from the same molecule, i.e., a H_2S^- , and that they correspond to para and ortho states of this molecule (Sec. IV). This establishes H_2S^- in KCl as a free or hindered quantum rotator. In Sec. V a rough analysis of the g and hyperfine components is given, confirming in a general way the conclusions of the preceding sections. In Sec. VI data on the HDS^- and D_2S^- centers are presented. Finally, a discussion of the data is presented in Sec. VII.

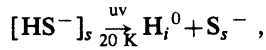
II. EXPERIMENTAL DETAILS

The KCl samples used in these experiments contained either SH^- or comparable amounts of SH^- and SD^- . They came from KCl boules grown in a 5-Torr atmosphere of H_2S or D_2S . The SH^- or SD^- concentrations

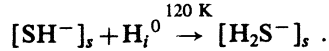
were estimated to be about 0.1 mol %. Some of the samples were the same as those used in the H^0Li^+ -center Raman investigations and contained Li^+ impurities.¹⁰ However, no effect of the Li^+ impurity is present in the defect investigated in this paper. The ESR procedures were the same as in Ref. 16.

III. ANALYSIS OF THE H_2S^- ESR SPECTRA

The center which we shall identify as a H_2S^- molecule is produced as follows. First, the H_i^0 interstitial hydrogen-atom centers (also called U_2 centers) are produced by irradiating a $\text{KCl}:\text{SH}^-$ sample at 20 K with the uv light of a deuterium lamp, filtered by a 206-nm broadband interference filter, for about 1 h:



where i and s indicate the interstitial and substitutional site, respectively. The characteristic H_i^0 ESR spectrum can be readily observed and monitored.^{17,18} Subsequently, the sample is warmed to 120 K for a few minutes. At this temperature the interstitial hydrogen atoms have become mobile and some of them are trapped by substitutional SH^- to form substitutional H_2S^- molecules:



In ESR one observes after such a treatment two simple spectra, which we shall show to be intimately related. One is a single anisotropic line (the singlet) and the other consists of three equidistant hyperfine (hf) lines of *equal intensities* (the triplet). Both possess axial symmetry around $\langle 111 \rangle$. An ESR spectrum showing the singlet and the triplet at 25 K for the static magnetic field

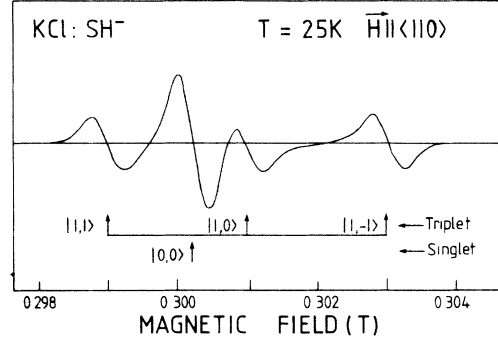


FIG. 1. The $\Theta=90^\circ$ ESR spectra of H_2S^- in $\text{KCl}:\text{SH}^-$ taken at 9.2 GHz and 25 K, and for the static magnetic field $\mathbf{H}||\langle 110 \rangle$. The singlet and the triplet lines are identified by the I, M_I values (see Fig. 5). The $\Theta=35.26^\circ$ spectra at higher fields are not shown.

$\mathbf{H}||\langle 110 \rangle$ is shown in Fig. 1, and in Table I are presented the parameters resulting from a fit to the spin Hamiltonian (usual notation)

$$\mathcal{H}_S/g_0\mu_B = g^{-1}\mathbf{H}\cdot\mathbf{g}\cdot\mathbf{S} + \mathbf{S}\cdot\mathbf{A}(\text{H})\cdot\mathbf{I}_H + \mathbf{S}\cdot\mathbf{A}({}^{33}\text{S})\cdot\mathbf{I}_S , \quad (1)$$

with $I_H=0$ for the singlet and $I_H=1$ for the triplet. The last term refers to the hf interaction with the nuclear spin $I_S = \frac{3}{2}$ ($\mu_N = 0.64274$ nuclear magnetons) of a single ${}^{33}\text{S}$ nucleus which has a 0.76% natural abundance. In Ref. 11 the ${}^{33}\text{S}$ hf interaction was determined in KCl samples containing 11.56% enriched ${}^{33}\text{SH}^-$ and these results are included in Table I. It is seen that the g parameters of the singlet and triplet spectra are very similar, although the g_1 values are clearly distinct.

TABLE I. The spin-Hamiltonian parameters of the H_2S^- , D_2S^- , and HDS^- centers in KCl at 25 K. The hydrogen, deuterium, and ${}^{33}\text{S}$ hyperfine parameters and the linewidth ΔH are given in mT. Note that the proton and deuterium hf values are not the principal hf values (see Sec. V C).

| Defect | | $g_{ }^a \langle 111 \rangle$ | g_1^a | $A_{ }(\text{H,D}) \langle 111 \rangle$ | $A_{\perp}(\text{H,D})$ | $A_{ }({}^{33}\text{S}) \langle 111 \rangle$ | $A_{\perp}({}^{33}\text{S})$ | ΔH |
|------------------------|----------------------|--------------------------------|---------|--|-------------------------|---|------------------------------|------------|
| H_2S^- | Singlet | 1.985 | 2.211 | | | | | |
| | Triplet | 1.986 | 2.206 | 3.29 ^c | 2.17 ^c | + 5.48 ^b | - 1.53 ^b | 0.40±0.05 |
| D_2S^- | Quintet ^d | 1.985 | 2.211 | 0.49 ^{e,c} | ~0.2 | | | ~0.5 |
| HDS^- | 6 K | 1.985 | 2.186 | 5.20 ^f | 4.07 ^f | | | ~0.6 |
| | 25 K | | | 3.85 ^f | 2.53 ^f | | | ~0.3 |

^aPrecision ±0.001.

^bFrom Ref. 11. The choice of signs is discussed in Sec. V B.

^cPrecision ±0.02 mT.

^dFor D_2S^- the g factors of the singlet, triplet, and quintet, and the hyperfine separation of the triplet and quintet, cannot be distinguished from one another.

^eThe deuterium triplet and quintet hf splitting; precision ±0.20 mT.

^fThe hydrogen hf splitting; precision ±0.1 mT. The hf splitting attributed to deuterium in Fig. 6 is not visible at 6 K; at 25 K one finds from $\mathbf{H}||\langle 111 \rangle$ that $A_{||}(\text{D})=0.41$ mT, but $A_{\perp}(\text{D})$ could not be determined (see text).

A second correspondence between the two spectra concerns their thermal formation and decay properties. These are shown in Fig. 2. It is seen from these normalized data that the production and decay of both centers coincide perfectly. Of course, the coincident formation may mean that both spectra are produced simultaneously through the decay of another center. Similarly, the coincident decay may mean either that both spectra are destroyed by a decaying center or that both spectra annihilate each other. However, the perfect coincidence of both curves and, particularly, the fact that the two spectra disappear completely and simultaneously strongly support the fact that both spectra originate from the same center.

The third and most significant fact confirms this. The relative intensities of the singlet and triplet change with the ESR observation temperature, the singlet being strongest at lower temperatures. The relative intensities are always the same at a given temperature in every sample, provided the microwave energy is kept sufficiently low (a few mW) in order to avoid saturation effects. It was indeed observed that the singlet line was somewhat more saturable at very low temperatures than the triplet.

If one plots the natural logarithm of the singlet/triplet intensity ratio versus $1/T$ in the temperature range 6–40 K, one obtains a straight line over more than a decade, as shown in Fig. 3. Clearly, the triplet grows at the expense of the singlet according to a Boltzmann distribution. The slope of this line corresponds to an energy of (16.2 ± 0.7) cm^{-1} and the conclusion is inescapable: The two ESR spectra originate from the same center, the singlet from the ground state and the triplet from an excited state at 16.2 cm^{-1} . This center is a substitutional H_2S^- molecule ion.

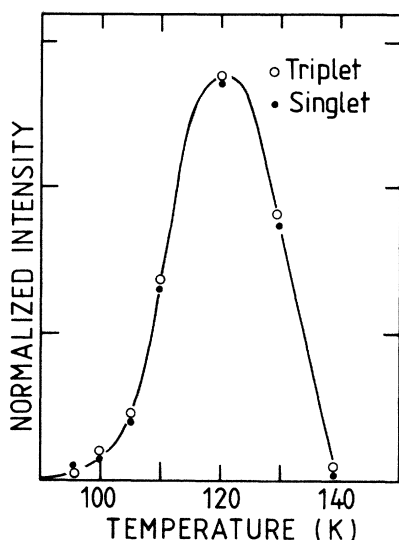


FIG. 2. The normalized formation and decay curves of the singlet and triplet lines of Fig. 1 as determined from a pulse-anneal experiment. At each temperature corresponding to a data point, the sample was held for 5 min and, subsequently, the changes in the ESR intensities were recorded at 25 K.

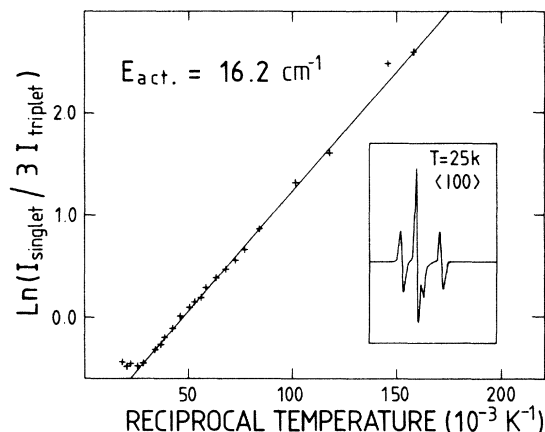


FIG. 3. Arrhenius plot of the relative intensity $I(\text{singlet})/3I(\text{triplet})$ of the H_2S^- ESR spectrum, showing that the triplet lines are enhanced at the expense of the singlet line, with an activation energy of 16.2 cm^{-1} . $I(\text{triplet})$ is the intensity of one of the triplet hf lines. These data were based on the $\Theta = 54.74^\circ$ spectra ($H \parallel \langle 100 \rangle$) in inset, but the same results were obtained from the $H \parallel \langle 110 \rangle$ spectra.

IV. THE ONE-DIMENSIONAL QUANTUM-ROTATOR MODEL

The above observations are straightforwardly explained by assuming that one is dealing with a H_2S^- molecule rotating around its C_{2v} axis, which is oriented along a $\langle 111 \rangle$ direction. As a result the H-H axis is perpendicular to the rotation axis and only the two protons determine the moment of inertia of the molecule. A schematic model of the center is presented in Fig. 4. Such a one-dimensional quantum rotator is described by

$$\mathcal{H}_{\text{rot}} = B_z J_z^2. \quad (2)$$

Here, J_z is the molecular angular momentum around the $\langle 111 \rangle$ -oriented rotation axis, and $B_z = \hbar^2/2I$ is the rotational constant, in which $I = \frac{1}{2}md^2$ is the moment of inertia, with m the proton mass and d the distance between the two protons. The energy levels are given by

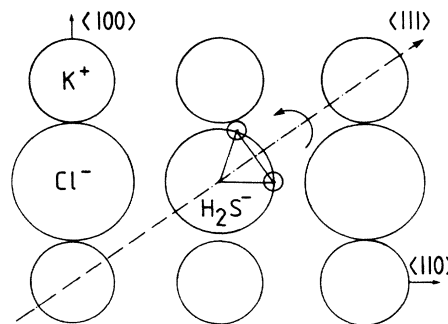


FIG. 4. Schematic model in a $\{110\}$ plane of the H_2S^- center in KCl, also showing the $z \parallel \langle 111 \rangle$ axis around which the molecule is rotating. The H-H distance is found to be $\sim 1.4 \text{ \AA}$ under the assumption that H_2S^- is freely rotating.

$$E(M_J) = B_z M_J^2, \quad (3)$$

and they are presented up to $M_J = \pm 2$ in Fig. 5.

In this quantum-rotator model the fermion character of the two indistinguishable H_2S^- protons play a dominant role. Briefly, the product of the molecular rotation wave function and the nuclear-spin wave function,

$$\Omega(M_J)\Psi(I, M_I), \quad (4)$$

must be antisymmetric under exchange of the two protons whose nuclear spins $\frac{1}{2}$ combine to $I=0, 1$. This leads to the *para* state

$$\Omega(M_J=0)\Psi(I=0, M_I=0),$$

which is a nuclear singlet, and the *ortho* state

$$\Omega(M_J = \pm 1)\Psi(I=1, M_I=0, \pm 1),$$

which is a nuclear triplet.

In the rotating H_2S^- model the *para* and *ortho* states are separated by B_z (Fig. 5). This should result in a dominant singlet line at low temperatures and a hf triplet, enhanced at the expense of the singlet, at higher temperatures. This corresponds exactly to the behavior of the experimentally observed singlet and triplet ESR lines (Fig. 3). This, together with the data of Sec. III, leaves no doubt that we are indeed observing a H_2S^- molecule which is rotating around a $\langle 111 \rangle$ direction. It will be demonstrated in Sec. V that the rotation axis is the C_{2v} axis of the molecule, as depicted in Fig. 4.

It may not be superfluous to emphasize that if the H_2S^- had been static in the crystal, or if it had been reorienting around a $\langle 111 \rangle$ axis through a sufficiently fast thermally activated jumplike motion, one would have observed in the ESR spectrum a hf triplet with intensity ratios 1:2:1 originating from the two equivalent protons. This would still be true even if the average reorientation rate would approach the rotation frequency of the free molecule as defined in the Introduction: a classically stochastically driven rotator is not a quantum rotator. Furthermore, because of its strong coupling to the lattice, a classically driven rotator will progressively shorten the spin-lattice relaxation time as its reorientation rate increases. It is unlikely under those circumstances that an ESR spectrum is observable when the average reorientation rate approaches the free reorientation frequency.

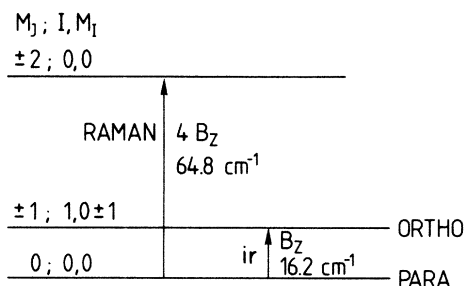


FIG. 5. Energy levels of the one-dimensional unhindered quantum rotator H_2S^- . The states, required to be antisymmetric for two protons, are indicated by the molecular rotation quantum number M_J and the nuclear-spin quantum numbers $I(0,1)$, M_I .

The result $B_z = 16.2 \text{ cm}^{-1}$ allows one to calculate the H-H distance in H_2S^- and one finds $d = 1.4 \text{ \AA}$. This may be compared to $d = 1.87 \text{ \AA}$ for the neutral H_2S molecule and 0.74 \AA for H_2 . Placing, as an approximation to the molecular structure, the two hydrogens on the surface of a S^- sphere (radius $\approx 1.35 \text{ \AA}$) yields a H-S-H angle of roughly 55° . In H_2S this angle is 92.2° .

V. DISCUSSION OF THE H_2S^- SPIN-HAMILTONIAN PARAMETERS

A. The g components

Because the spin-orbit interaction of sulfur ($\lambda = 170 \text{ cm}^{-1}$) is so much larger than that of hydrogen (which is only a few wave numbers), the contributions to the H_2S^- g shifts originate solely from those parts of the ground and excited molecular orbitals that are centered on the sulfur. Following Herzberg,²⁰ the molecular ground configuration of H_2S^- is $\dots (1b_2)^2(3a_1)^2(1b_1)^2(4a_1)^1$, with $2b_2$ the next unoccupied orbital. The $4a_1$ is composed out of an antibonding combination of an $s-p_z$ hybrid on the sulfur on one hand and $s-p$ hybrids on the two hydrogens on the other. The z axis is along the twofold axis and the y and x axes are in, and perpendicular to, the molecular plane, respectively. It is clear from the symmetry of H_2S^- that $g_x \neq g_y$. However, because of the rapid rotation, $g_\perp = \frac{1}{2}(g_x + g_y)$ is observed.

The molecular orbitals contributing in first order to g_\perp are the occupied orbitals $1b_1$ (with a p_x on the sulfur) and $1b_2$ (with a p_y on the sulfur) and the unoccupied antibonding $2b_2$. The latter gives a negative contribution to g_\perp while the former two contribute positively. The net result is a positive g shift $g_\perp - g_0$. There is no first-order contribution to g_\parallel . The three orbitals contribute negatively in second order to both g_\perp and g_\parallel , resulting, in particular, in a negative shift $g_\parallel - g_0$. This is in agreement with experimental g -factor data presented in Table I. A more quantitative discussion is useless at this point because too many parameters occur in the theoretical expressions.

Finally, the fact that the singlet and the triplet have slightly different g_\perp values illustrates the contribution of the spin-rotation interaction^{7,8,21} to the g_\perp factor of the triplet state.

B. The ^{33}S hyperfine interaction

The sizable g shifts indicate that for a reliable quantitative analysis of the ^{33}S hyperfine interaction it is necessary to include higher-order contributions in the theoretical expressions of the hyperfine components. For atoms, which possess only a single force center, the higher-order contributions can be expressed in terms of the experimental g shifts,²² and the same is true for molecules in which all the constituent atoms are equivalent.²³ The latter is clearly not the case for the H_2S^- molecule. However, because one is in the favorable position here that the g shifts are exclusively determined by the sulfur part of the molecular orbital (see Sec. V A), the higher-order contributions can be approximately expressed as a function of the shifts $\Delta g_i = g_0 - g_i$, provided one makes the additional assumption that the amounts of sulfur p orbitals are roughly com-

parable to each other in the $1b_1$, $1b_2$, $4a_1$, and $2b_2$ molecular orbitals. This is not an unreasonable assumption, but it could be a rough approximation. It is also a necessary approximation at this point if one wants to make progress in the quantitative analysis. The formulas derived in Ref. 22 for a p^1 configuration are applicable to the complementary p^5 configuration of S⁻ and, consequently, we will use the following expressions to analyze the ³³S hyperfine components:

$$A_{||} = A_{\sigma}(1 - 1/2\Delta g_{||}) + (2 + 3/2\Delta g_{\perp} + 1/2\Delta g_{||})\rho, \quad (5)$$

$$A_{\perp} = A_{\sigma}(1 - 1/2\Delta g_{||}) - (1 + 13/4\Delta g_{\perp} - 9/4\Delta g_{||})\rho.$$

In these formulas,

$$\rho \equiv \rho(\text{H}_2\text{S}^-) = \alpha^2 \rho(\text{S}^-) \equiv \alpha^2 \frac{2}{5} (\mu_I/I) \langle r^{-3} \rangle_{3p} \quad (6)$$

is the anisotropic contribution of a S⁻ $3p$ electron to the hyperfine interaction and A_{σ} the isotropic one. The latter can be written as

$$A_{\sigma} \equiv A_{\sigma}(\text{H}_2\text{S}^-) = \alpha^2 A_{\sigma}^e(\text{S}^-) + A_{\sigma}^s, \quad (7)$$

in which $A_{\sigma}^e(\text{S}^-)$ is the exchange-polarization contribution to the hf interaction of the free S⁻ ion, and

$$A_{\sigma}^s = \beta^2 (8\pi/3) (\mu_I/I) |\psi_{3s}(0)|^2$$

the contribution caused by s mixing on the sulfur in the H₂S⁻ ground state.

In Eqs. (6) and (7), α^2 represents the amount of sulfur $3p_z$ orbital in the molecular H₂S⁻ ground state. Because s mixing is usually very small ($\beta^2 \ll \alpha^2$), α^2 gives the unpaired electron density on the sulfur part of the molecule.

Using the data of Table I, with the particular choice made for the signs of the ³³S hf components which give the best agreement with theory (see below), one derives from Eqs. (5) that

$$\rho \equiv \rho(\text{H}_2\text{S}^-) = +3.5 \text{ mT}, \quad A_{\sigma} \equiv A_{\sigma}(\text{H}_2\text{S}^-) = -0.5 \text{ mT}. \quad (8)$$

It is interesting to compare these results with the corresponding parameters of the S⁻ ion. The ESR spectrum of the substitutional S⁻($3p^5$) ion in the alkali halides was analyzed in Ref. 15. The threefold orbital degeneracy is lifted through a D_{2h} Jahn-Teller (JT) distortion of the surroundings, leaving the unpaired hole in a $3p_z$ orbital oriented along a $\langle 110 \rangle$ direction. The S⁻ ESR data are (in an axial approximation)

$$g_z = 1.9073, \quad A_z(^{33}\text{S}) = -2.47 \text{ mT}, \quad (9)$$

$$g_{\perp} = 2.4142, \quad A_{\perp}(^{33}\text{S}) = +4.29 \text{ mT},$$

where again we have made the choice of signs of the hf components that give the best agreement with the theoretical ρ value (see below). Applying Eqs. (5) to these data yields the following results:

$$\rho(\text{S}^-) = +7.7 \text{ mT}, \quad A_{\sigma}(\text{S}^-) = -7.0 \text{ mT}. \quad (10)$$

Because the substitutional S⁻ center possesses inversion symmetry and no s mixing can occur, the A_{σ} value in (10) must correspond to the A_{σ}^e value of the free S⁻ ion. It is seen that the value $A_{\sigma}^e = -7.0 \text{ mT}$ is large and negative.

The S⁻($3p^5$) ion shares this property with the np^1 ($n=4,5,6$) heavy-metal atoms and ions (Ref. 22).

The $\rho(\text{S}^-)$ value calculated from (6) using²⁴ $\langle r^{-3} \rangle_{3p} = 35 \times 10^{24} \text{ cm}^{-3}$ of S⁻ yields $\rho(\text{S}^-) = +7.6 \text{ mT}$, which is in good agreement with (10) and justifies the choice of the signs of the hf components made in (9) for S⁻ and in Table I for H₂S⁻.

From (6), (8), and (10) the amount of unpaired electron density on the sulfur part of H₂S⁻ is found to be

$$\alpha^2 = 0.45, \quad (11)$$

which means that about half of the electron density resides on the sulfur. This is not an unreasonable result.

From (10) and (11) one calculates that

$$\alpha^2 A_{\sigma}^e(\text{S}^-) = A_{\sigma}(\text{H}_2\text{S}^-) = -3.2 \text{ mT},$$

which does not agree with the experimental value $A_{\sigma}(\text{H}_2\text{S}^-) = -0.5 \text{ mT}$ given in (8). As a result, one concludes from (7) that the difference is due to s mixing by an amount

$$A_{\sigma}^s = +2.8 \text{ mT}.$$

The foregoing g and ³³S hf analysis is consistent with our assumption (Sec. IV) that $4a_1$ is the ground-state orbital of H₂S⁻ and that the axis around which the rotation takes place is the $\langle 111 \rangle$ -oriented C_{2v} axis. Note that, because it is taking place around the C_{2v} axis along which the sulfur $3p_z$ lobe is oriented, the rotation does not affect the measured ³³S hyperfine interaction.

C. The proton hyperfine interaction

In contrast to the ³³S case treated above, the molecular rotation does influence the measured proton hf interaction. From the point of view of ESR and for a static H₂S⁻ molecule, the two protons are inequivalent with respect to the static magnetic field \mathbf{H} , unless \mathbf{H} lies either along the proton-proton axis or in a plane perpendicular to the molecular plane and going through the C_{2v} axis. The hf tensor axes of the two protons do not coincide. In an axial approximation the two proton hf axes are oriented along the directions of the s - p hybrids on the hydrogens. As a result, the proton hf values quoted in Table I do *not* constitute the principal values of the hf tensors. At this point they merely represent the hf separations measured parallel and perpendicular to the C_{2v} axis. A proper analysis has to take the rotational motion into account and must be performed along the lines presented in Refs. 25–27. In order for such an analysis to be successful, exceedingly accurate hf measurements have to be performed for a sufficient number of orientations of the magnetic field \mathbf{H} with respect to the molecule. Such an analysis would yield interesting structural information about the H₂S⁻ molecule, such as, e.g., the H-S-H angle. Unfortunately, our attained accuracy did not warrant such an analysis and none was attempted.

VI. THE D₂S⁻ AND HDS⁻ CENTERS

In a KCl crystal containing a mixture of SH⁻ and SD⁻ impurities, the D₂S⁻ and HDS⁻ centers are formed to-

gether with H_2S^- when one follows the production procedure as given in Sec. III. These species are readily identified in ESR through their characteristic hf pattern and temperature behavior. ESR spectra for $\text{H}||\langle 111 \rangle$ and at 25 K are presented in Fig. 6. An angular variation shows that, similar to H_2S^- , the D_2S^- center possesses axial symmetry around $\langle 111 \rangle$.

The D_2S^- molecule should also be freely rotating around its $\langle 111 \rangle$ -oriented C_{2v} axis. Because deuterons are spin-1 bosons, the rotation–nuclear-spin product function (4) should be symmetric under exchange of the two nuclei. This leads to the following allowed states: a nuclear quintet

$$\Omega(M_J=0)\Psi(I=2, M_I),$$

a nuclear singlet

$$\Omega(M_J=0)\Psi(I=0, M_I),$$

and a nuclear triplet

$$\Omega(M_J=\pm 1)\Psi(I=1, M_I).$$

At the lowest ESR measuring temperatures ($T=6$ K) the D_2S^- hf quintet is clearly visible and it decreases as the temperature is raised. The D_2S^- singlet ESR line cannot be distinguished from the overlapping H_2S^- singlet. In any case, the quintet and singlet constitute the molecular ground manifold of D_2S^- , but how much splitting there is between them and which of the two is the actual ground state depends on the specific interaction between the two nuclear spins. The separation is, however, expected to be very much smaller than B_2 .

The spin-Hamiltonian parameters as determined from the quintet are presented in Table I. The observed $A_{||}(\text{H})/A_{||}(\text{D})$ hyperfine ratio between H_2S^- and D_2S^- is 6.7 ± 0.3 , which is comfortably close to the 6.52 ratio de-

rived from the nuclear moments. This is not so for the A_{\perp} ratio. Barring a deeper analysis of the hyperfine components (see Sec. V C), this deviation could be caused by a low-accuracy A_{\perp} determination for D_2S^- . Because the lines overlap each other strongly, it is not possible to make an Arrhenius analysis of the triplet/quintet intensity ratio of D_2S^- , and the corresponding rotational splitting $B_2(\text{D}_2\text{S}^-)$ could not be determined. Scaling the H_2S^- result by mass leads to $B_2(\text{D}_2\text{S}^-)=8.1 \text{ cm}^{-1}$ if the D-D distance is taken the same as the H-H separation.

For the HDS^- molecule, nuclear-spin statistics do not play a role and one expects a straightforward ESR pattern: two hydrogen ($I=\frac{1}{2}$) hf lines, each of which is further split into a superhyperfine triplet originating from interaction with the deuterium nucleus ($I=1$).

Such a spectrum is observed at 25 K (see Fig. 6) with a hydrogen hf splitting that is very similar to the H_2S^- case (see Table I), and a deuterium triplet splitting (0.41 mT for $\text{H}||\langle 111 \rangle$), which again is comparable to the D_2S^- case. However, when the temperature is lowered to 6 K this spectrum decreases in intensity and a hydrogen hf doublet with a substantially increased splitting grows, each component possessing a 0.6-mT linewidth and showing no discernible deuterium splitting (Table I). The angular variation of the H and D hf separation is difficult to analyze because of the low resolution of the ESR spectra. Again, as was already pointed out in Sec. V C, motional effects must be taken into account in a proper analysis of these data.

VII. DISCUSSION AND CONCLUSIONS

The observation in ESR of the para and ortho states of the H_2S^- molecule in KCl, and the analysis of the g parameters and the hydrogen and ^{33}S hyperfine structure, proves that the molecule is rotating around its C_{2v} axis, which is oriented along a $\langle 111 \rangle$ direction. The question arises whether it is freely rotating or to what extent it is experiencing a hindering potential of C_{3v} symmetry. Turning on a hindering potential of increasing strength will progressively reduce the rotation frequency, until at a certain point it is more appropriate to speak of a tunneling reorientation motion. The transition is a gradual one, but one essential thing remains the same: the motion is in both cases coherent, i.e., the time dependence of the states s is given by a simple exponential $\exp(i\omega_s t)$. Furthermore, the importance of the nuclear-spin statistics in determining the symmetry of the molecular states remains in the tunneling case. Qualitatively, the two regimes cannot be distinguished.

If an independent determination of the H-H distance d in H_2S^- were available, one would be able compare the calculated moment of inertia with the one derived from the experimental rotational constant $B_2=16.2 \text{ cm}^{-1}$. However, such information is not available. As a result, little can be said about the absence or presence of a hindering potential on H_2S^- . The value $d=1.4 \text{ \AA}$ derived in Sec. III for the H-H distance is an upper limit and corresponds to the case of genuine free rotation of H_2S^- . A hindering potential will lead to a smaller value for d . A lower limit is undoubtedly set by the internuclear distance

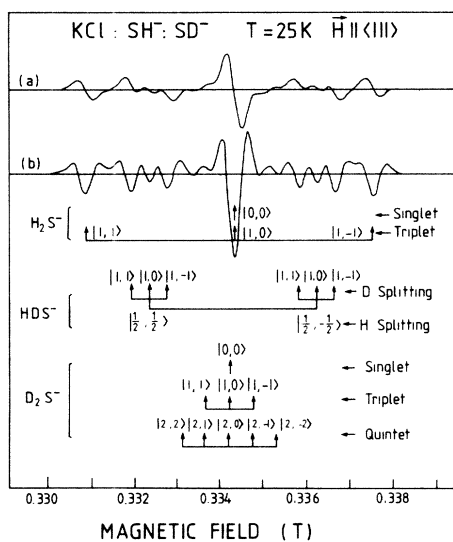


FIG. 6. X-band ESR spectra of H_2S^- , D_2S^- , and HDS^- in KCl containing comparable amounts of SH^- and SD^- , at 25 K for $\text{H}||\langle 111 \rangle$. (a) The first derivative and (b) the second derivative of the spectra are presented.

$d=0.78 \text{ \AA}$ of molecular H₂ because it corresponds to an exclusively covalent bond between two hydrogen atoms. It is expected that in H₂S⁻ the hydrogens are preferentially bonded to the S⁻. In any case, the distance should be smaller than $d=1.87 \text{ \AA}$ in neutral H₂S, and this is indeed the case.

In molecular hydrogen the conversion of the metastable ortho-H₂ to the stable para-H₂ modification is a slow one, taking many months in the absence of a suitable catalyst.³ In contrast, the para to ortho transition in H₂S⁻ is a fast one. Clearly, because of the interaction of the protons with the magnetic moment of the unpaired electron spin, which is itself strongly coupled to the lattice, the two nuclear-spin states can be, and are, rapidly converted into one another.

The fact that the singlet and triplet lines possess distinctly different g_{\perp} factors is caused, via the spin-rotation interaction, by the large sulfur spin-orbit interaction. In lighter rotating molecules, such as NH₂ or CH₃, these effects are not resolved. The singlet from triplet separation has, as an isolated fact, led in earlier work¹¹ to the conclusion that they belong to different species. The demonstration in this paper that the singlet line also originates from a H₂S⁻ molecule, rather than from a S⁻ center of D_{3d} symmetry along $\langle 111 \rangle$, settles a problem that has led to considerable confusion.¹²⁻¹⁵ Instead of having to accept the existence of two stable Jahn-Teller-distorted configurations, i.e., D_{3d} and D_{2h} , for a substitutional S⁻ ion in alkali halides it is now clear that there is only one, namely the S⁻ center possessing D_{2h} symmetry along $\langle 110 \rangle$ (or C_{2v} along $\langle 110 \rangle$ if the possibility of an off-center S⁻ is considered), as discussed in Ref. 15.

It would clearly be interesting to study the analogous H₂O⁻ center in OH⁻-doped alkali halides. A center

designated as such was identified in ENDOR (electron-nuclear double resonance) some time ago,²⁸ but it was established, and confirmed in later studies,²⁹⁻³² that this center is better described as being a neutral H₂O molecule embedded in a F center ("the wet F center"). In other words, the extra electron is not bound to the molecule as it is H₂S⁻, but it is delocalized over the surrounding ions. Still, the ENDOR measurements indicate the presence of interesting motional properties of the H₂O molecule inside the F center, and in view of the results presented in this paper it might be interesting to reanalyze these spectra. The study of the properties of both the H₂S⁻ and H₂O⁻ centers under applied uniaxial stress would undoubtedly yield interesting information about their motional properties.

Finally, we have attempted to measure the Raman spectrum of the H₂S⁻ molecule. The $M_j=0$ to $M_j=2$ transition is Raman active and should be at $4B_z=64.8 \text{ cm}^{-1}$ for a completely unhindered H₂S⁻ rotator. Deviations from this value would give an idea about how much the rotator is hindered. However, a careful search failed to yield a scattering signal in this region. Undoubtedly, the concentration and the Raman scattering cross section are both too low.

ACKNOWLEDGMENTS

The authors would like to thank L. O. Schwan and J. M. Spaeth for supplying some of the crystals used in these experiments, and A. Bouwen for experimental support. This work was supported by IIKW (Interuniversitair Instituut voor Kernwetenschappen) and the Geconcerteerde Acties (Ministerie van Wetenschapsbeleid), to which the authors are greatly indebted.

*Permanent address: Tsi Huang University, Beijing, China.

¹V. Narayanamurti and R. O. Pohl, *Rev. Mod. Phys.* **42**, 201 (1970).

²F. Lüty and J. Ortiz-Lopez, *Phys. Rev. Lett.* **50**, 1289 (1983).

³I. F. Silvera, *Rev. Mod. Phys.* **52**, 393 (1980).

⁴G. Herzberg, *Electronic Spectra of Polyatomic Molecules* (Van Nostrand/Reinhold, New York, 1966).

⁵S. Clough and F. Foldy, *J. Chem. Phys.* **51**, 2076 (1969).

⁶H. M. McConnell, *J. Chem. Phys.* **29**, 1422 (1958).

⁷For a recent survey of the ESR spectra of rotating molecules, see W. Weltner, Jr., *Magnetic Atoms and Molecules* (Van Nostrand/Reinhold, New York, 1983).

⁸I. Bojko and R. H. Silsbee, *J. Magn. Reson.* **5**, 339 (1971).

⁹R. H. Silsbee and I. Bojko, *J. Phys. Chem. Solids* **34**, 1971 (1973).

¹⁰W. Joosen, J. F. Zhou, E. Goovaerts, and D. Schoemaker, *Phys. Rev. B* **31**, 6709 (1985).

¹¹A. Hausmann, *Z. Phys.* **192**, 313 (1966).

¹²B. Eilebrecht and L. Schwan, *J. Phys. (Paris) Colloq.* **37**, O7-162 (1976).

¹³A. S. Abhvani, S. P. Austen, and C. A. Bates, *Solid State Commun.* **37**, 777 (1981).

¹⁴H. Bill, D. Döhner, L. Schwan, and E. Sigmund, *Solid State Commun.* **34**, 383 (1983).

¹⁵L. E. Vannotti and J. R. Morton, *Phys. Rev.* **174**, 448 (1968).

¹⁶E. Goovaerts, J. Andriessen, S. Nistor, and D. Schoemaker,

Phys. Rev. B **24**, 29 (1981).

¹⁷F. Kerkhoff, W. Martienssen, and W. Sander, *Z. Phys.* **173**, 184 (1963).

¹⁸J. M. Spaeth and M. Storm, *Phys. Status Solidi* **42**, 739 (1970).

¹⁹G. Herzberg, *Infrared and Raman Spectra of Polyatomic Molecules* (Van Nostrand/Reinhold, New York, 1945).

²⁰*Electronic Spectra of Polyatomic Molecules*, Ref. 4, p. 317.

²¹A. Carrington and D. H. Levy, *Adv. Chem. Phys.* **18**, 149 (1970).

²²D. Schoemaker, I. Heynderickx, and E. Goovaerts, *Phys. Rev. B* **31**, 5687 (1985); I. Heynderickx, E. Goovaerts, and D. Schoemaker, *Solid State Commun.* **55**, 887 (1985).

²³D. Schoemaker, *Phys. Rev. B* **7**, 786 (1973).

²⁴E. Clementi, *IBM J. Res. Dev.* **9**, 2 (1965).

²⁵D. Schoemaker, *Phys. Rev. B* **3**, 3516 (1971).

²⁶D. Schoemaker and E. L. Yasaitis, *Phys. Rev. B* **5**, 4970 (1972).

²⁷W. Van Puymbroeck and D. Schoemaker, *Phys. Rev. B* **23**, 1670 (1981).

²⁸W. Rush and H. Seidel, *Solid State Commun.* **9**, 231 (1971).

²⁹S. P. Morato and L. Gomes, *J. Phys. (Paris) Colloq.* **41**, C6-155 (1980).

³⁰S. P. Morato and F. Lüty, *Phys. Rev. B* **22**, 4980 (1980).

³¹W. Kuch and U. Durr, *J. Phys. Chem. Solids* **42**, 677 (1981).

³²L. Gomes and S. P. Morato, *Solid State Commun.* **41**, 653 (1982).